

## Experimental investigation for wheel polygonisation of high-speed trains

Qu, Sheng; Zhu, Bin; Zeng, Jing; Dai, Huanyun; Wu, Pingbo

**DOI**

[10.1080/00423114.2020.1772984](https://doi.org/10.1080/00423114.2020.1772984)

**Publication date**

2020

**Document Version**

Final published version

**Published in**

Vehicle System Dynamics

**Citation (APA)**

Qu, S., Zhu, B., Zeng, J., Dai, H., & Wu, P. (2020). Experimental investigation for wheel polygonisation of high-speed trains. *Vehicle System Dynamics*, 59(10), 1573-1586.  
<https://doi.org/10.1080/00423114.2020.1772984>

**Important note**

To cite this publication, please use the final published version (if applicable).  
Please check the document version above.

**Copyright**

Other than for strictly personal use, it is not permitted to download, forward or distribute the text or part of it, without the consent of the author(s) and/or copyright holder(s), unless the work is under an open content license such as Creative Commons.

**Takedown policy**

Please contact us and provide details if you believe this document breaches copyrights.  
We will remove access to the work immediately and investigate your claim.

# Experimental investigation for wheel polygonisation of high-speed trains

Sheng Qu, Bin Zhu, Jing Zeng, Huanyun Dai & Pingbo Wu

To cite this article: Sheng Qu, Bin Zhu, Jing Zeng, Huanyun Dai & Pingbo Wu (2021) Experimental investigation for wheel polygonisation of high-speed trains, Vehicle System Dynamics, 59:10, 1573-1586, DOI: [10.1080/00423114.2020.1772984](https://doi.org/10.1080/00423114.2020.1772984)

To link to this article: <https://doi.org/10.1080/00423114.2020.1772984>



Published online: 31 May 2020.



Submit your article to this journal [↗](#)



Article views: 268



View related articles [↗](#)



View Crossmark data [↗](#)



Citing articles: 3 View citing articles [↗](#)



# Experimental investigation for wheel polygonisation of high-speed trains

Sheng Qu<sup>a</sup>, Bin Zhu<sup>a,b</sup>, Jing Zeng<sup>a</sup>, Huanyun Dai<sup>a</sup> and Pingbo Wu<sup>a</sup>

<sup>a</sup>State Key Laboratory of Traction Power, Southwest Jiaotong University, Chengdu, People's Republic of China; <sup>b</sup>Section of Road and Railway Engineering, Faculty of Civil Engineering and Geosciences, Delft University of Technology, Delft, The Netherlands

## ABSTRACT

The wheel polygonisation is the harmonic wave along the wheel circumference, which has been widely reported in high-speed railway vehicles in China in recent years. The polygonization mechanism has not been fully understood yet, and this work discusses one possible mechanism through several experiments. Firstly, a field test for the CRH3 high-speed train with polygonal wheels is carried out. It is found that the vibration in vertical takes major responsibility, and there are several resonance bands for the train-track system. Another field test shows that the rail is sensitive to the polygonisation characteristic frequency, but the wheel axle is not. Then the rail local vibration modes are analyzed by the operational deflection shape (ODS) test in the laboratory. A loaded bogie is fixed on the tested track to simulate the real working conditions. The result shows that the frequency of one local mode is 591 Hz, which is a typical wheel polygonisation frequency. Besides, the wheel-rail contact point is not on the vibration node of this local mode. Thus, the resonance of this local rail mode can be one possible mechanism for the high-order wheel polygonisation.

## ARTICLE HISTORY

Received 11 February 2020  
Revised 14 April 2020  
Accepted 17 May 2020

## KEYWORDS

Wheel polygonisation;  
experimental proof; axle-box  
acceleration; local resonance

## 1. Introduction

### 1.1. Different types of polygonisation

The wheel polygonisation does not mean the wheel should be polygonal, and it is defined as harmonic irregularities around the wheel tread circumference. The wheel polygonisation was noticed several decades ago in the railway industry. Moreover, most of them are reported to be low-order polygonisation due to the low vehicle operation speed [1–5].

In recent years, with the rapid development of the high-speed railway network in China, a large number of structural failures have been reported to be connected to the wheel polygonisation [6,7]. Different from the traditional train, the wavelength of the harmonic irregularity found on the high-speed train wheels are much shorter. According to reports of China's railway operation department and some previous researches [8,9], the polygonisa-

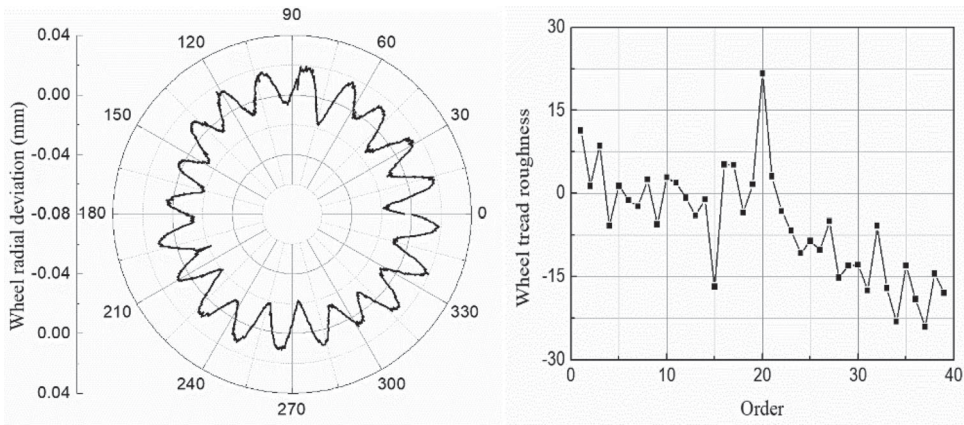


**Figure 1.** A typical 20th-order wheel polygonisation measured on a Chinese high-speed train. The running speed of this train is about 300 km/h, currently the maximum commercial speed in China. (The left is the roughness of the wheel circumference. The right is the harmonic order of the roughness, and the y-axis is roughness level  $L_r^k$ , which is defined as  $L_r^k = 10 \times \log_{10}(r_k^2/r_{ref}^2)$ ,  $r_k$  is the wheel radial deviation and  $r_{ref}$  is set as  $1\mu m$ )

tion order on the high-speed wheel is closely related to the operating speed. For the trains at an operating speed of 250 and 300 km/h, the dominant orders are 23–24th and 18–20th, respectively. Interestingly, the polygonisation passing frequency has no apparent connection with the operating speed level, and they always focus on the range of 550–600 Hz. Furthermore, according to the literature [9], the polygonisation order is dominated by the operating speed, and lightly influenced by the wheel diameter.

Figure 1 displays a typical measured wheel polygonisation (radial deviation) in a polar coordinate and its harmonic order components. The harmonic order should be calculated from the Fourier series of the radial deviation rather than merely counting from the wheel radial deviation. Generally, the high-order polygonisation has a small amplitude, which is no more than 0.1 millimetre. However, the axle-box impact acceleration can reach a high level of more than 100 g due to the high vehicle speed. With the frequency up to about 600 Hz, vehicle track components are vulnerable to fatigue damage in a short period. Therefore, the research on polygonisation is of considerable significance to reduce maintenance costs and ensure the operation safety.

## 1.2. Different views on high-order polygonisation

Some theories have been proposed to explain the formation mechanism of the high-order wheel polygonisation found on the high-speed trains. One of the popular opinions is provided by Jin and his group [3,6,7,10–11]. Jin and Wu [7] carried out a field test on a high-speed train equipped with 23th-order polygonal wheels. They found that the polygonisation induced passing frequency (590 Hz) is coincident with the natural frequencies of the bogie frame and wheelset, 589 and 601 Hz respectively. However, the hammer test and simulation show that no natural frequency of the track is closed to 590 Hz. So, they believed that it is the wheelset and bogie resonance, rather than the vibration of the track, that should be mainly responsible for the high-order polygonisation.

Wang and Dai et al. [12–14] investigated a large number of high-speed train wheels. They found that the bogie wheelbase determines the wheel polygonisation induced frequency. The frequency and the wheel radius decide the order of the polygonisation. Experiments and simulations show that ‘rail third-banding mode resonance’ is the main reason for the high-order polygonisation.

The researches focusing on the formation of high-order wheel polygonisation are not many.

Some other researchers provided different perspectives on general wheel polygonisations, which can be applied to the study on the high-order wheel polygonisation. For instance, Chi [15] studied the polygonisation problem by a data-driven approach, and found that the polygonisation is more likely to appear in summer. Ye [16] found the wheel flat could develop into polygonisation.

The wheel-rail contact force and stiffness are high, which means that the interaction between the wheelset and rail in the high-frequency domain is considerable. So, it is arbitrary to analyze the vibration mode of an isolated rail to seek for the resonance frequencies and ignore the interaction with the wheelset, vice versa. What is agreed is that the high-order wheel polygonisation is frequency-fixed. From the viewpoint of this paper, the vehicle-track structure should be treated as a whole system, and the polygonisation is caused by the resonance of one local vibration mode. In this paper, several experiments are carried out to analyze the polygonisation mechanism. The structure of this paper is illustrated as follows.

In section 2, A field test of a typical high-speed trains CRH3 is carried out. Vibrations in different directions are analyzed. Different natural frequencies bands of the system are pointed out. Furthermore, it is found that vibration components of around 600 Hz are outstanding when an impact excitation is transmitted through the rail.

In section 3, The operational deflection shape (ODS) analysis for the rail is performed to indicate the local vibration modes and resonance frequencies of the rail.

In section 5, Discussions and conclusions will be made.

## 2. Field test on polygonisation

### 2.1. Test introduction

The amplitude of the high-order polygonisation is tiny, usually smaller than 0.1 mm, seen in Figure 1. As a result, it is not easy to distinguish the polygonisation by human eyes. However, the high noise reported by the driver and the structural failure indicates its existence. For instance, bolts failures have been reported to be found on the tested trains.

When the vehicle runs on the track, the excitation of the system is made up of two parts. One is the periodical out-of-roundness of the wheel, and the other is the stochastic rail irregularity. Under such excitation, the dynamics response of the wheelset or rail is crucial to understand the problem of the wheel polygonisation, which is highly suspected to be caused by abnormal vibration. Considering the feasibility, the wheelset vibration measurement is performed instead of the track vibration measurement. The wheel-rail force caused by the non-smooth contact surfaces will directly excite the vibration of the wheel. However, the wheel rotates at a very high speed, and it is challenging to set sensors on the wheel axle. The mass of the axle-box is relatively small compared to the wheel, and the

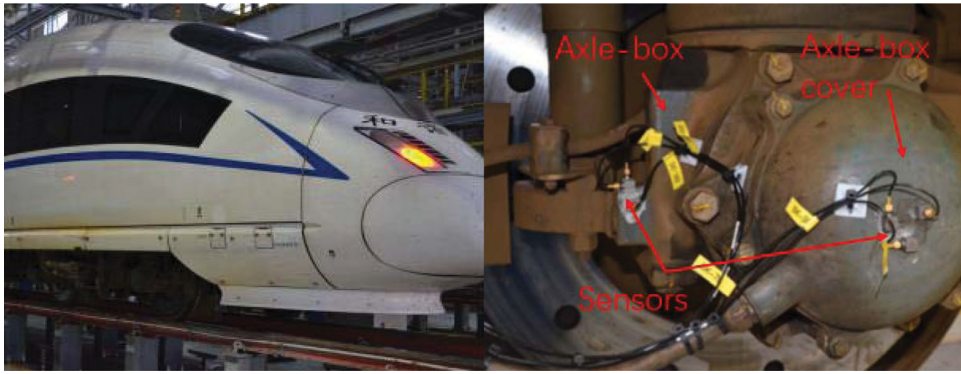


**Figure 2.** The tested CRH3 high-speed train and the acceleration sensors in different directions on the axle-box.

assembling of the bearing is tight. It is reasonable to believe that the acceleration of the axle-box is consistent with that of the wheel axle. Given this reason, the vibration data of the wheel can be easily acquired by measuring the acceleration of the axle-box, as showing in Figure 2. In the test system, GPS sensors are also installed synchronously to get the speed and position information.

The polygonisation have been found on the wheels of the tested train CRH3, which is developed from the ICE 3, and some improvements have been made to make it better adapt to China's track system. During the test, the tested train ran from the Guangzhou city to Wuhan city with passengers on it. The maximum operating speed is 300 km/h, and the total test mileage is 1068 kilometers. In this way, the real working condition of the train is guaranteed. It is noticed that almost all the tested Guangzhou-Wuhan high-speed line is CSRT I double-block ballastless track. Only a very small party is built as other types of ballastless track, while no ballast track is used in this line. The track type will be discussed later.

## 2.2. Data acquirement

After being equipped with sensors mentioned above, the tested trains are put into commercial operation to guarantee the reliability of the test data. Figure 3 shows the full view of the axle-box vertical acceleration from Guangzhou to Wuhan.

It is seen in Figure 3 that there are eight stops (cities) in the test. The departure and arrival cities are Guangzhou and Wuhan, respectively. The speed data shows that CRH3 running speed mainly distributes in a narrow range of about 300 km/h except for the acceleration and deceleration section. The axle-box acceleration increases with the vehicle speed, and when the speed reaches 300 km/h, the axle-box acceleration goes up to about 50 g.

### 2.2.1. Vertical and lateral vibration

The volume of the test data is large due to the high sampling frequency (5000 Hz) and the extended test time. Considering the data volume and the GPS integrity, the data from Xianning to Wuhan city is chosen to do analysis. Moreover, another reason for picking out

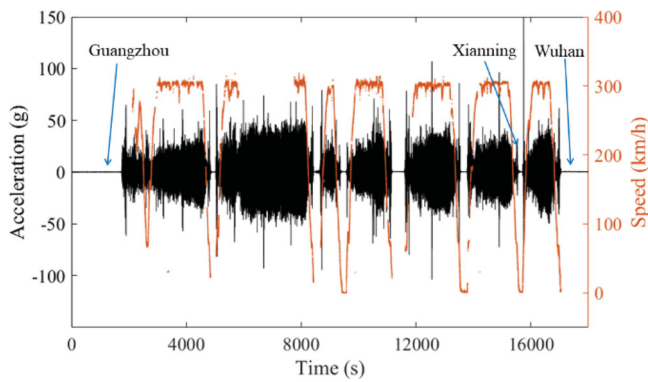


**Figure 3.** The vertical acceleration and speed overview of the tested train.

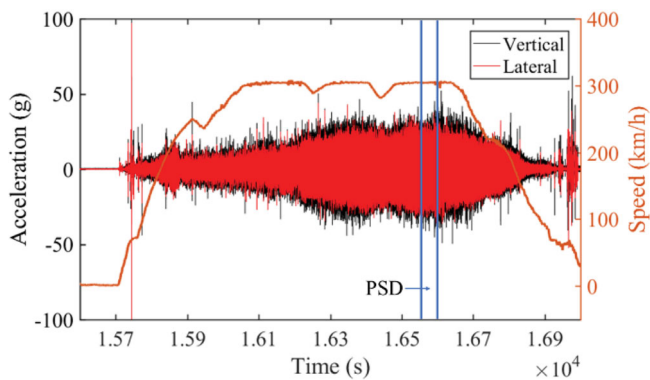


**Figure 4.** The lateral and vertical acceleration of the axle-box in the time domain.

this section is that there are different track types in this section. According to the literature [17], the lateral motion of the whole wheelset contributes to the low-order polygonisation (with 1,2,4 harmonic OOR orders). For the high-order polygonisation, the vibrating direction will be discussed in this section. The lateral and vertical axle-box accelerations of the tested CRH3 are compared in the time domain and frequency domain.

As shown in Figure 4, both the vertical and lateral acceleration fluctuate with the vehicle speed. The vertical acceleration is distinctly larger than the lateral acceleration, and both are generally less than 50 g. The power spectral density (PSD) of the acceleration in 80 s are calculated when the vehicle speed is steady at 300 km/h. Figure 5 shows the PSD of the selected acceleration data between the two blue lines in Figure 6. Considering the main polygonisation order (20th), the vehicle speed (84.2 m/s) and the wheel radius (0.459 m), it can be calculated that the highest peak of the PSD (585.4 Hz) is the polygonisation passing frequency. Notably, the y-axis is logarithmic, the component of 585.4 Hz is dominant compared with other components.

For the lateral vibration, the components around 700 Hz (Part 4 in Figure 5 a) are outstanding, the component at polygonisation passing frequency is relatively high but still neglectable compared to the vertical vibration. Furthermore, no other peaks can be easily picked out, which means that the lateral vibration mainly appears as stochastic vibration.

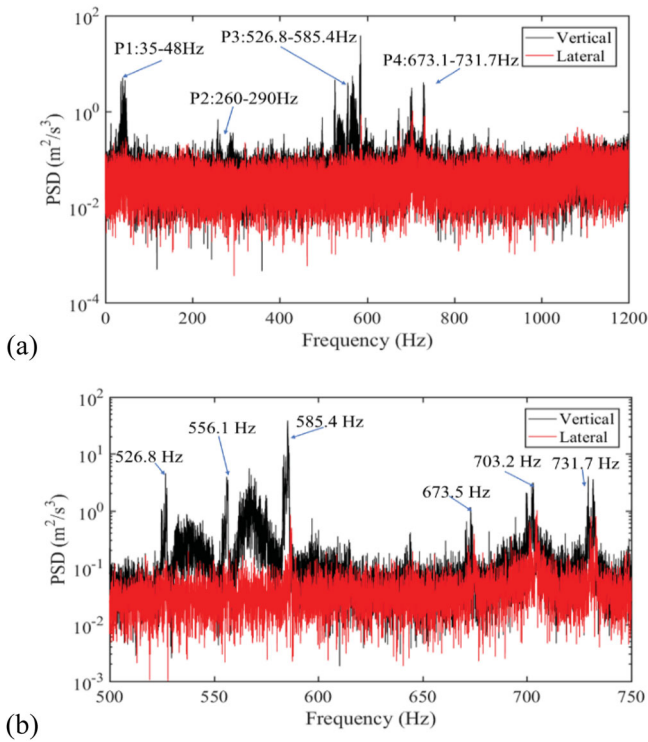


**Figure 5.** The lateral and vertical acceleration of the axle-box in the frequency domain. (b is a part of a).

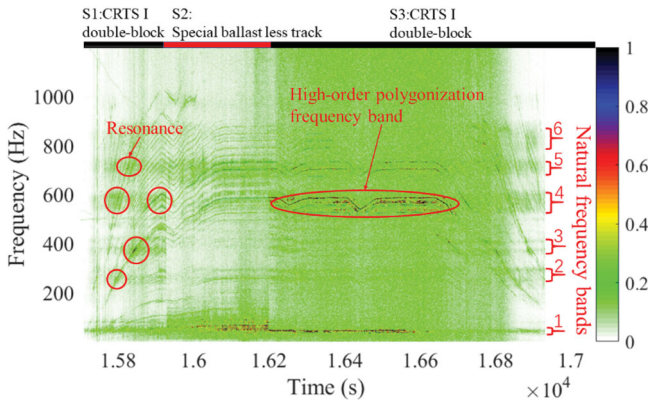


**Figure 6.** The short-time Fourier transform of the acceleration data from Xianning to Wuhan.

For the vertical direction, the vibration power mainly distributes at four parts marked in Figure 5 (a). The first part (35–48 Hz) is related to P2 force, and the magnitude of the second part from 260 Hz to 290 Hz is relatively neglectable. As for the fourth part (673.5–731.7 Hz), the vertical vibration is coincident with the lateral vibration. The vertical vibration power mainly distributes at the third part from 526.8–585.4 Hz. Within the polygonal characteristic frequency range (around 585.4 Hz), there are no comparable lateral vibration components. Moreover, lateral vibration is only sensitive to frequencies

around 700 Hz. It indicates that lateral vibration is not a direct factor in the formation of high-order polygonisation. The peak frequencies in Figure 5 (b) are equal to the exact multiples of the wheel rotation frequency (29.2 Hz). These peaks are caused by the periodical wheel irregularities.

### 2.2.2. Polygonisation mechanism analysis

The chosen data from Xianning to Wuhan is very valuable because most of this high-speed line is CRTS I double-block ballastless track, but in this section, a small part of the track is different. Thus, the influence of the track structure can be studied. The short-time Fourier transform is introduced to analyze the acceleration data in time and frequency domain. The result is shown in Figure 6.

Seen in Figure 6, the axle-box acceleration mainly consists of two types of components, one is the relatively narrow component, which fluctuates exactly with the vehicle speed, and the frequencies of these peaks always equal to the multiples of the wheel rotational frequency. It means that the irregularities of the wheel cause this kind of vibration component, and it acts as the primary excitation. The other type is the relatively wide frequency band, whose frequency remains invariable as the vehicle speed changes. As shown on the right side of Figure 6, there are six distinct frequency bands for the CRTS I double-block track. Different from the wheel irregularity induced frequencies, this type of component is independent of the running speed. They are the natural frequencies of the track-wheel coupled structure.

In track section 1, the wheel irregularity induced frequencies (excitation frequencies) become higher as the train speed up. When the excitation frequencies reach the natural frequency bands, resonance peaks as marked in Figure 6 can be found. As the wheel speed continues to increase, the excitation frequency exceeds the natural frequency band, and the resonance peaks disappear.

When the train runs at a speed of 300 km/h on track section 3, the frequency bands 2,3,6 are covered by the white noise. As for the natural frequency band 1 (35–48 Hz), high-order polygonisation cannot propagate under such an excitation, because of its low frequency. Moreover, it is not the integral multiple of the wheel rotational frequency. For the natural frequency band 5, its vibration power is significantly lower than that of band 4. While the vibration power in the frequency band from 556 to 585 Hz is dominant compared to other frequency components. The highest resonance peak can be found at the frequency of 585.4 Hz, which is caused by the 20th polygonisation. As the speed increase, the polygonisation induced frequency passes the frequency band 1,2,3 and reaches band 4. The resonance peak at the band 4 is significantly higher than the peaks at other frequency bands. It is reasonable to believe that the polygonisation is highly related to the resonance vibration around 585 Hz. The vibration modes at around 585 Hz should be identified.

Another distinct phenomenon is that the track structure is crucial to the dynamic response of the axle-box. In Figure 6, there are distinct boundaries between the two different types of tracks. In track section 2, it is easy to recognise that the frequency bands 2,4,5 are similar to those of track section 1 and 3. However, its vibration power distribution pattern in the frequency domain is considerably different from that of other track sections. The frequency band 1 became much wider, and the band 3 disappears. It means that the frequency bands 1 and 3 are closely related to the track structure under the rail.

It can be concluded that the high-order polygonisation is frequency-fixed. There are many natural frequency bands of the vehicle-track coupled system. The vehicle-track structure determines the natural frequency bands and their sensitivity to excitation. At the same time, the vehicle speed determines the frequency pattern of the excitation. Structure and speed together determine the vibration energy distribution in the frequency domain. It can be speculated that the more concentrated the vibration energy distribution, the easier the polygonisation will propagate.

### 2.2.3. Weak proof of the rail causing mechanism

In the previous section, the resonance at the natural frequency band around 600 Hz is found to be related to the formation of the polygonisation. This section will discuss the source of this natural frequency band. The vibration source could form two parts, namely the vehicle and the track. Furthermore, the vibration of the wheelset and rail are supposed to play a major role in wheel polygonal wear, because the structures above the wheelset and below the rail are separated from the wheel-rail contact pair by the primary suspension and fastener rubber. So, this section focuses on the wheelset and rail vibration at around 600 Hz.

The idea of the experiment is explained as follows. The wheel tread is newly reprofiled, and the rail top surface is supposed to be smooth. It means that the axle-box acceleration data will not contain the frequency components caused by the wheel tread and rail top irregularities. If the wheel runs over a defect on the right rail, a pulse excitation will be applied to the right wheel and right rail. Two sensors are set on the left and right axle-boxes of the rear wheelset, respectively. By acquiring the data of the right sensor when the front wheel runs over the defect, the transmissibility of the rail at 600 Hz can be defined. Analogously, by assessing the data of the left sensor when the rear wheel runs over the defect, the transmissibility of the wheelset at 600 Hz can be defined. Finally, by comparing the transmissibility of the rail and the wheelset, their contributions to wheel polygonisation can be determined. Figure 7 shows the vertical acceleration of the left and right axle box in one second. The peaks are supposed to be caused by rail defects. As there are some

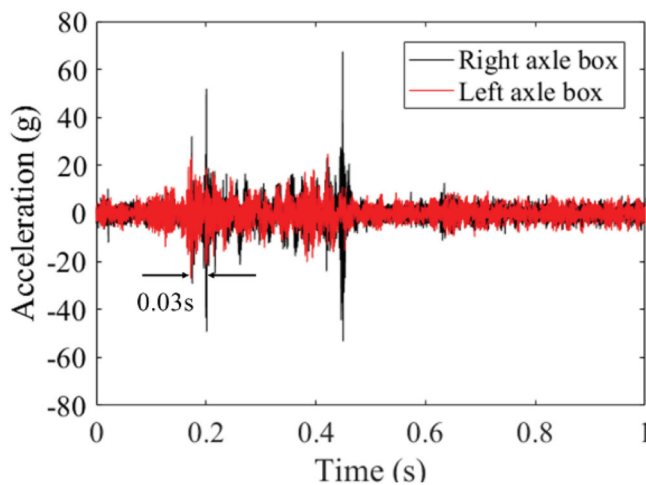


**Figure 7.** The vertical acceleration of the left and right axle box in one second.

assumptions and uncertain test conditions in this experiment, so this section is called ‘weak proof’.

Generally, the acceleration of the reprofiled wheel is under 10 g, which is much lower than that of the polygonal wheel. The two impact peaks at 0.17 and 0.20 s are caused by the rail defect. The time interval between the two peaks is 0.03 s. Considering the running speed of 83.3 m/s, the spatial distance of the two peaks is 2.5 metres, which is precisely the wheelbase of the tested bogie. In this test, sensors are set at the rear wheelset of the bogie. It can be inferred that the first peak is caused by the front wheel passing the rail defect, the rear sensor collected the signal because the impact vibration is transmitted to the rear wheelset through the rails. Corresponding peaks can be found on the left wheel axle-box, although their amplitudes are distinctly lower than those of the right wheel. It can be explained as the impact vibration is transmitted to the left wheel axle-box though the wheel axle. The impact transmission though the rail and wheel axle can be marked as the rail vibration and the wheel vibration under the impact excitation, respectively.

The frequency band around 585 Hz is the characteristic frequency range of the high-order polygonisation. The rail defect induced impact force can be considered as a broad-band pulse. By checking the vibration in the frequency domain, the vibration form can be obtained. Due to the short time period, the wavelet technique is introduced to ensure frequency resolution. Figure 8 shows the wavelet analysis results of the acceleration mentioned in Figure 7.

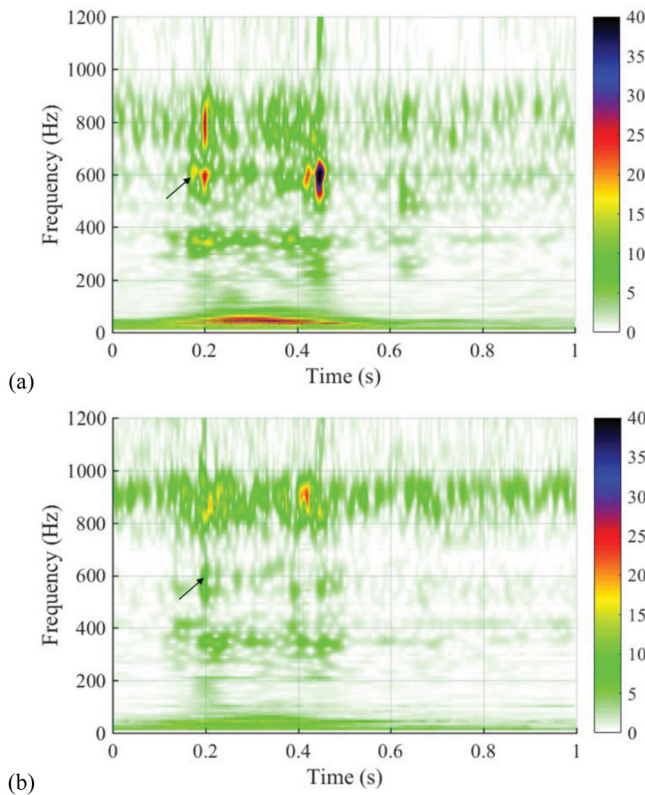


**Figure 8.** Wavelet analysis of the vertical acceleration. (a) The right axle-box, (b) the left axle-box.

In Figure 8(a), outside the rail defect impact area (e.g. 0.5–1 s), there are no outstanding vibration components around the frequency of 585 Hz. At 0.17 s, the front wheel is passing the rail defect, the vibration transmits to the rear wheel through the rail and recorded by the sensor. As the arrow shows, the component around 600 Hz is dominating. This vibration component agrees well with the polygonisation characteristic frequency. At 0.2 s, the rear wheelset (tested wheelset) is passing the rail defect, the vibration around 600 Hz is still outstanding, and some other frequency components can also be observed. In Figure 8(b), at 0.2 s, the rail defect induced vibration transmit to the left wheel through the wheel axle. However, no distinct frequency component can be observed around the polygonisation frequency. Conclusions can be drawn from the above analysis, that the rail should be responsible for the vibration near the polygonisation characteristic frequency.

### 3. Operational deflection shape (ODS) analysis

In section two, the rail vibration is found to be sensitive to the frequency around 600 Hz. In this section, an operational deflection shape (ODS) experiment will be carried out to find the possible local vibration mode of the rail.

#### 3.1. Test method

The static load for the wheel-rail pair of a high-speed train is about 60–80 kN. The contact stiffness can reach a level of about 1.25 MN/mm according to the contact mechanics. By such a high contact stiffness, the wheel and the rail can significantly interact with each other, especially in the high-frequency domain. As a result, the vibration mode and the natural frequency of the wheelset-track coupled structure will be significantly different from an isolated track (without the load of a train). The above is the reason why the polygonisation characteristic frequency cannot be found in the hammer test of an isolated track in previous works [7].

To take the vehicle into consideration, a mode test of the bogie-track coupled structure is carried out to seek for the polygonisation characteristic frequency in the Traction Power Laboratory (TPL) in Chengdu. The bogie is from a CRH 3C high-speed train, which once served on the Wuhan-Guangzhou high-speed line. A force of 24 kN is applied to the top of the air spring of the bogie to simulate the gravity of the car body. The bogie wheelbase is 2.5 m. The track in the test is the CTRS-I (double-block sleepers ballastless track), which is the same track as the Wuhan-Guangzhou high-speed line. The sleeper span of the track is 0.65 m. Fifteen acceleration sensors are set evenly along the side of the rail head under the bogie. The sensor range and sampling rate are 700 g and 5000 Hz, respectively. The tested bogie-track structure is shown in Figure 9. The exciting point is in the middle of the rail between the two wheels.

#### 3.2. ODS analysis

The experimental ODSs analysis data for the local rail vibration are plotted in Figures 10 and 11. A hammer is used to obtain a white noise input, and the responses of the rail are analyzed in the frequency domain. The test is repeated eight times. Figure 10 shows the linear spectrum for the rail acceleration of the fifteen tested locations. As can be seen in



**Figure 9.** The tested bogie-track system in laboratory and the acceleration sensors.

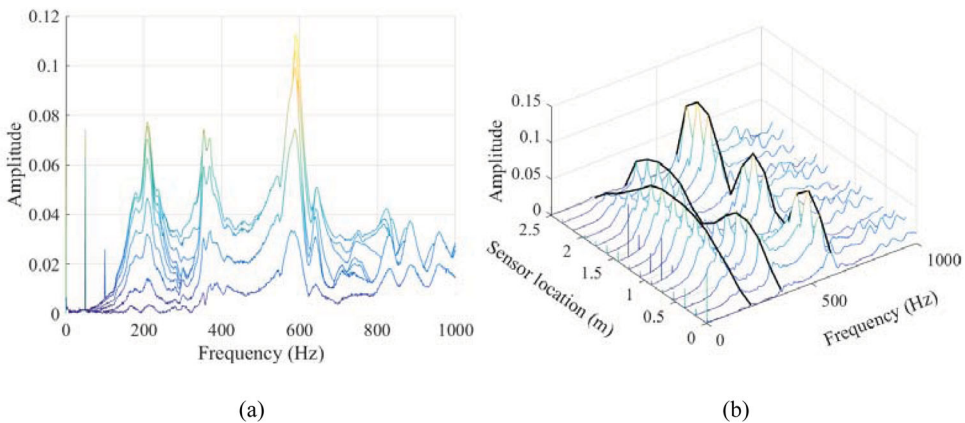


**Figure 10.** (a) Linear spectrum for the rail acceleration in fifteen different locations. (b) The solid black lines connect two adjacent peaks.

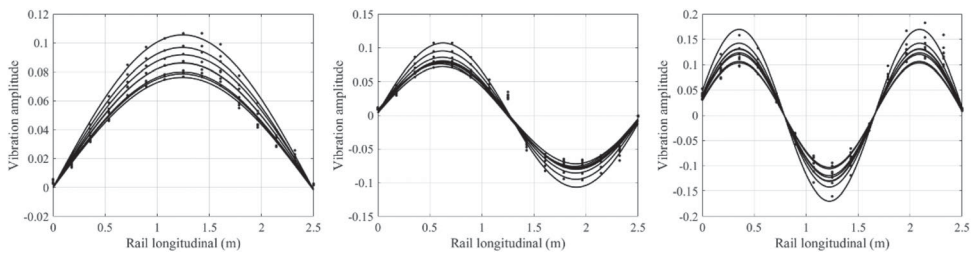


**Figure 11.** Experimental ODSs of the rail (dots) at different frequencies and their fitting curves. (From the left to the right, the frequencies of the ODSs are 209, 352 and 591 Hz, respectively)

Figure 10(a), the third peak is the highest among the peaks. Furthermore, its frequency is 591 Hz, which agrees well with the peak in Figure 8 and the polygonisation characteristic frequency as well. The linear frequency spectrum is arranged as the spatial coordinates of the sensors, and the maximum vibration amplitude of the rail at different frequencies can be easily identified. In Figure 10(b), the two wheels of the bogie are located at 0 and 2.5 metres. The three peaks of 209, 352, and 591 Hz match the one, two, and three half-sine waves between the two wheels, respectively.

**Table 1.** Details about the experimental local modes.

	Frequency		Average	Standard deviation
Alpha	209 Hz	Wave length (m)	4.9719	0.0022
		Phase (m)	0.0003	0.0029
Beta	352 Hz	Wave length (m)	2.6396	0.0035
		Phase (m)	0.0895	0.0187
Gamma	591 Hz	Wave length (m)	1.7740	0.0061
		Phase (m)	0.3434	0.0060

Furthermore, considering the vibration phases of the sensors, the ODSs at different frequencies can be obtained. The dots in Figure 11 show the ODSs of the rail in the eight tests, and the solid lines are fitted from the dots by harmonics. The fitting function is set as follows.

$$y = A \sin(\omega x + \varphi) \quad (1)$$

Where  $\varphi$  is the spatial phase of each vibration mode in Table 1. The wavelength of each mode can be calculated by  $2\pi/\omega$ . It can be seen that the distance between the excitation point and the vibration node point equals to  $\varphi$  divided by  $\omega$ .

In Figure 11, the ODSs tests are performed eight times. From the ODS perspective, it is reasonable to consider that the local vibration modes of the rail are harmonics, and lines can be considered as the rail local modes between the wheels of a bogie. The spatial wavelength and the spatial phases of the vibration modes show high repeatability. Although their amplitudes are different from each other, it does not influence the rail local vibration modes. Here, the local modes at 209, 352 and 591 Hz are marked as modes Alpha, Beta, and Gamma, respectively. These modes are not called as 1st, 2nd and 3rd bending modes in this paper, because they are just defined in a local scale. The rail length can be infinitely long in the field. There must be vibration modes with lower natural frequencies considering the system in a larger scale. The details about the experimental local modes are listed in Table 1.

It is seen in Table 1, the standard deviations of the experimental parameters are small, showing high repeatability of this experiment. The wavelengths of the local rail modes are closely related to the wheelbase of the bogie (2.5 m). The wavelength of Alpha mode is twice the length of the wheelbase, and the wavelength of Beta mode equals to the wheelbase. The spatial phases of the Alpha and the Beta modes are closed to 0 m, which means that the wheel-rail contact force acts at the vibration nodes of the Alpha and Beta mode. Because wheel-rail contact force is the only excitation for the rail vibration, and the vibration nodes are motionless in this vibration mode. Therefore, the Alpha and Beta modes resonance cannot be easily excited. It is notable that in Table 1, different from the Alpha and Beta modes, the wavelength of Gamma mode is larger than two-thirds of the wheelbase. A distinct spatial phase of 0.34 m can be found in the mode Gamma. In other words, the excitation force does not act at the vibration nodes of the Gamma mode. This could be the reason why mode Gamma is easier to be excited. Thus, the local rail mode Gamma resonance can be one explanation to the peaks around 600 Hz in Figure 6 and Figure 8(a). Furthermore, why the spatial phase of mode Gamma is larger than the other two modes could be further discussed. It may be related to the mode stiffness of the rail. The mode stiffness of the mode Gamma is higher than other modes due to shorter wavelength, which means that its mode stiffness is closer to the high wheel-rail contact stiffness. As a result,

rail Gamma mode vibration is more likely to couple with the wheel-rail contact. Wheel-rail contact vibration will distance the contact point from the vibration node, so the phase appears.

In literature [8], similar rail local bending modes are solved by simulation. However, there are some differences compared to the views of this work. The characteristic frequencies are different. Moreover, literature [8] explained that the polygon frequency is consistent with the 'third mode', but is different from other modes because the 'third mode' has a higher amplitude and frequency.

#### 4. Conclusion and discussion

In this work, the data of three experiments are provided to find a possible explanation for the high-speed train wheel polygonisation. The field tests are carried out on a commercial operated high-speed train. A wealth of information can be obtained through the analysis of the axle-box acceleration data in both time and frequency domain. Finally, an ODS test of the rail is performed in the laboratory. The conclusions can be drawn as follows.

The polygonisation passing frequency of the tested train is 585.4 Hz under an operating speed of 300 km/h. The polygonisation is highly related to the vertical vibration, while it has little to do with the lateral vibration.

The train-track system has six distinct natural frequency bands that can be distinguished by the axle-box acceleration. Typical polygonisation frequency happens to be in the 4th natural frequency band. Once a polygonisation is formed, a strong resonance occurs.

When a wheel-rail impact pulse transmitted by the rail, the vibration component of about 600 Hz will dominate. However, no 600 Hz component can be easily recognised when the wheel transmits the pulse. The vibration of the wheel-rail coupling system at 600 Hz is mainly performed by the rail.

ODS test shows that the local rail mode Gamma has a natural frequency of 591 Hz, which agrees well with the polygonisation frequency. Moreover, the vibration nodes of this local mode do not locate at the wheel-rail contact point. As a result, this mode can be excited more easily than other modes. The ODS test gives a novel explanation about why the rail local mode Gamma dominates the rail vibration, but the testing is under a static load limited by the laboratory testing condition. More rigorous improvements could be done in future works, such as the rail ODS test with a full-speed vehicle in the field.

In conclusion, when there are some initial irregularities on the wheel tread, the wheel-rail contact force will have components of the wheel rotational multiple frequencies. If one of these frequencies is close to the natural frequency of the local rail mode Gamma, polygonisation will propagate.

#### Acknowledgments

This work is supported by the National Natural Science Foundation of China (grant number 11790282, 51805451, 51975485), Independent Research and Development Project of the State Key Laboratory of Traction Power (Grant number: 2019TPL-T18).

#### Disclosure statement

No potential conflict of interest was reported by the author(s).

## Funding

This work was supported by National Natural Science Foundation of China: [Grant Number 11790282,51805451,51975485]; State Key Laboratory of Traction Power: [Grant Number 2019TPL-T18].

## References

- [1] Kaper HP. Wheel corrugation on Netherlands railways (NS): origin and effects of “polygonization” in particular[J]. *J Sound Vib.* 1988;120(2):267–274.
- [2] Meywerk M. Polygonalization of railway wheels[J]. *Arch Appl Mech.* 1999;69(2):105–120.
- [3] Jin X, Wu L, Fang J, et al. An investigation into the mechanism of the polygonal wear of metro train wheels and its effect on the dynamic behaviour of a wheel/rail system[J]. *Veh Syst Dyn.* 2012;50(12):1817–1834.
- [4] Li W, Li Y, Zhang X, et al. Mechanism of the polygonal wear of metro train wheels[J]. *Chin J Mech Eng.* 2013;49(18):17–22.
- [5] Johansson A, Andersson C. Out-of-round railway wheels—a study of wheel polygonalization through simulation of three-dimensional wheel–rail interaction and wear[J]. *Veh Syst Dyn.* 2005;43(8):539–559.
- [6] Jin X-s. Key problems faced in high-speed train operation. Singapore: China’s High-Speed Rail Technology, Springer; 2018; 27–45.
- [7] Wu Y, Du X, Zhang H-j, et al. Experimental analysis of the mechanism of high-order polygonal wear of wheels of a high-speed train. *J Zhejiang Univ Sci.* 2017;18(8):579–592.
- [8] Wu X, Rakheja S, Cai W, et al. A study of formation of high order wheel polygonalization. *Wear.* 2019;424–425:1–14.
- [9] Cai W, et al. Experimental and numerical analysis of the polygonal wear of high-speed trains. *Wear.* 2019;440:203079.
- [10] Zhang J, et al. Influence of wheel polygonal wear on Interior noise of high-speed trains. Singapore: China’s High-Speed Rail Technology, Springer; 2018; 373–401.
- [11] Tao G, Wang L, Wen Z, et al. Experimental investigation into the mechanism of the polygonal wear of electric locomotive wheels. *Veh Syst Dyn.* 2018;56(6):883–899.
- [12] Dai H, Li D, Zhuang S. Study on the mechanism of high order out of round and wear of high-speed railway train’s wheel. *Dynamics of Vehicles on Roads and Tracks Vol 2.* Rockhampton: CRC Press; 2017; p. 1321–1327.
- [13] Wang J, et al. Long-term vibration evolution of China CRH3 series high speed trains. *Dynamics of Vehicles on Roads and Tracks Vol 2.* Rockhampton: CRC Press; 2017; p. 1315–1320.
- [14] Wang J, Song C, Wu P, et al. Wheel reprofiling interval optimization based on dynamic behavior evolution for high speed trains. *Wear.* 2016;366–367:316–324.
- [15] Chi Z, Lin J, Chen R, et al. Data-driven approach to study the polygonization of high-speed railway train wheel-sets using field data of China’s HSR train. *Measurement.* 2020;149:107022.
- [16] Ye Y, et al. Wheel flat can cause or exacerbate wheel polygonization. *Veh Syst Dyn.* 2019: 1–30. doi:10.1080/00423114.2019.1636098
- [17] Morys B. Enlargement of out-of-round wheel profiles on high speed trains[J]. *J Sound Vib.* 1999;227(5):965–978.